Available online at www.sciencedirect.com
ScienceDirect
Journal of Molecular Catalysis A: Chemical 272 (2007) 249–257
JOURNAL OF MOLECULAR CATALYSIS A: CHEMICAL
www.elsevier.com/locate/molcata

Selective oxidation of cyclohexene to di-2-cyclohexenylether by host (nanocavity of zeolite-Y)/guest (manganese(II) complexes with 12- and 14-membered tetraazaz tetraone macrocyclic complexes) nanocomposite materials (HGNM)

Masoud Salavati-Niasari [a,b,*]

[a] *Institute of Nano Science and Nano Technology, University of Kashan, P.O. Box 87317-51167, Kashan, Iran*
[b] *Department of Chemistry, University of Kashan, P.O. Box 87317-51167, Kashan, Iran*

Received 6 March 2007; received in revised form 17 March 2007; accepted 20 March 2007
Available online 24 March 2007

Abstract

Manganese(II) complexes of [12]aneN$_4$: 1,4,7,10-tetraazacyclododecane-2,3,8,9-tetraone; [14]aneN$_4$: 1,4,8,11-tetraazacyclotetradecane-2,3,9,10-tetraone; Bzo$_2$[12]aneN$_4$: dibenzo-1,4,7,10-tetraazacyclododecane-2,3,8,9-tetraone; Bzo$_2$[14]aneN$_4$: dibenzo-1,4,8,11-tetraazacyclotetradecane-2,3,9,10-tetraone have been encapsulated in the nanopores of zeolite-Y by the in situ one pot template condensation reaction. Mn(II) complexes with azamacrocyclic ligand were entrapped in the nanocavity of zeolite-Y by a two-step process in the liquid phase: (i) adsorption of [bis(diamine)manganese(II)]; [Mn(N–N)$_2$]–NaY; in the supercages of the zeolite, and (ii) in situ condensation of the manganese(II) precursor complex with diethyloxalate. The new host–guest nanocomposite materials (HGNM) have been characterized by FTIR, DRS and UV–vis spectroscopic techniques, XRD and elemental analysis, as well as nitrogen adsorption. These complexes (neat and HGNM) were used for oxidation of cyclohexene with *tert*-butylhydroperoxide (TBHP) as oxidant in different solvents. Di-2-cyclohexenylether was identified as main product. 2-Cyclohexen-1-one and 2-cyclohexene-1-ol were obtained as minor products. Also it was found [Mn(Bzo$_2$[12]aneN$_4$)]$^{2+}$–NaY in ethanol had the highest reactivity (84.51%), although the selectivity was 95.10% towards the formation of ether product in methanol.

Keywords: Nanoporous material; Oxidation of cyclohexene; Azamacrocycle; Manganese(II)

1. Introduction

IUPAC classifies porous materials into three categories: (1) microporous with pores of less than 2 nm in diameter, (2) mesoporous having pores between 2 and 50 nm, and (3) macroporous with pores greater than 50 nm. The term nanoporous materials have been used for those porous materials with pore diameters of less than 100 nm. Many kinds of crystalline and amorphous nanoporous materials such as framework silicates and metal oxides, zeolites, pillared clays, nanoporous silicon, carbon nanotubes and related porous carbons have been described lately in the literature [1].

Nanoporous materials are exemplified by crystalline framework solids such as zeolites, whose crystal structure defines channels and cages, i.e. nanopores, of strictly regular dimensions. They can impart shape selectivity for both reactants and the products when involved in the chemical reactions and processes. The large internal surface area and void volumes with extremely narrow pore size distribution as well as functional centers homogeneously dispersed over the surface make nanoporous solids highly active materials. Over the last decade, there has been a dramatic increase in synthesis, characterization and application of novel nanoporous materials [2].

Zeolites, which represent the largest group of nanoporous materials, are crystalline inorganic polymers based on a three-dimensional arrangement of SiO_4 and AlO_4 tetrahedra connected through their oxygen atoms to form large negatively charged lattices with Brønsted and Lewis acid sites. These negative charges are balanced by extra-framework alkali and/or alkali

* Correspondence address: Department of Chemistry, University of Kashan, P.O. Box 87317-51167, Kashan, Iran. Tel.: +98 361 5555 333; fax: +98 361 555 29 30.
E-mail address: salavati@kashanu.ac.ir.

1381-1169/$ – see front matter © 2007 Elsevier B.V. All rights reserved.
doi:10.1016/j.molcata.2007.03.049

earth cations. The most-known zeolites are silicalite-1, ZSM-5, zeolite beta and zeolites X, Y, and A. The incorporation of small amounts of transition metals into zeolitic frameworks influences their properties and generates their redox activity. Zeolites with their well-organised and regular system of nanopores and nanocavities also represent almost ideal matrices for hosting nanosized particles, e.g., transition metal complexes that can also be involved in catalytic applications.

Nanoporous encapsulated metal complexes are mostly used as heterogeneous and redox catalysts in petroleum industry and in the production of chemicals for various types of shape-selective conversion and separation reactions [3]. They form the basis of new environment-friendly technologies, involving cheaper, more efficient and more environment-friendly ways for carrying out chemical reactions. Transition metal-modified nanoporous molecular sieves with aluminosilicate frameworks catalyze wide variety of synthetically useful oxidative transformations with clean oxidants such as hydrogen peroxide or molecular oxygen under relatively mild conditions with the advantage of facile recovering and recycling, if compared to homogeneous liquid phase catalyst, like sulphuric acid [4–6].

In this paper, I report the synthesis and characterization of manganese(II) complexes of 12- and 14-membered tetraaza macrocyclic ligand; [12]aneN$_4$: 1,4,7,10-tetraazacyclododecane-2,3,8,9-tetraone; [14]aneN$_4$: 1,4,8,11-tetraazacyclotetradecane-2,3,9,10-tetraone; Bzo$_2$[12]aneN$_4$: dibenzo-1,4,7,10-tetraazacyclododecane-2,3,8,9-tetraone and Bzo$_2$[14]aneN$_4$: dibenzo-1,4,8,11-tetraazacyclotetradecane-2,3,9,10-tetraone; encapsulated within the nanopores of zeolite-Y by the template condensation of diethyloxalate and [bis(diamine) manganese(II)]; [Mn([12]aneN$_4$)]$^{2+}$–NaY, [Mn([14]aneN$_4$)]$^{2+}$–NaY; [Mn(Bzo$_2$[12]aneN$_4$)]$^{2+}$–NaY; [Mn(Bzo$_2$[14]aneN$_4$)]$^{2+}$–NaY; shown in Schemes 1 and 2 and used in the oxidation of cyclohexene with *tert*-butylhydroperoxide (TBHP) as oxygen donor (Scheme 1 and 2).

2. Experimental

2.1. Materials and physical measurements

All other reagents and solvent were purchased from Merck (pro-analysis) and dried using molecular sieves (Linde 4 Å). Cyclohexene was distilled under nitrogen and stored over molecular sieves (4 Å). Cyclohexanone was used as an internal standard for the quantitative analysis of the product using gas chromatography. Reference samples of 2-cyclohexene-1-ol and 2-cyclohexene-1-one (Aldrich) were distilled and stored in the refrigerator. *tert*-Butlhydroperoxide; TBHP; (solution 80% in di-*tert*-butylperoxide) were obtained from Merck Co. NaY with the Si:Al ratio of 2.53 was purchased from Aldrich (Lot no. 67812). FT-IR spectra were recorded on Shimadzu Varian 4300 spectrophotometer in KBr pellets. The electronic spectra of the neat complexes were taken on a Shimadzu UV–vis scanning spectrometer (Model 2101 PC). Diffuse reflectance spectra (DRS) were registered on a Shimadzu UV/3101 PC spectrophotometer the range 1500–200 nm, using MgO as ref-

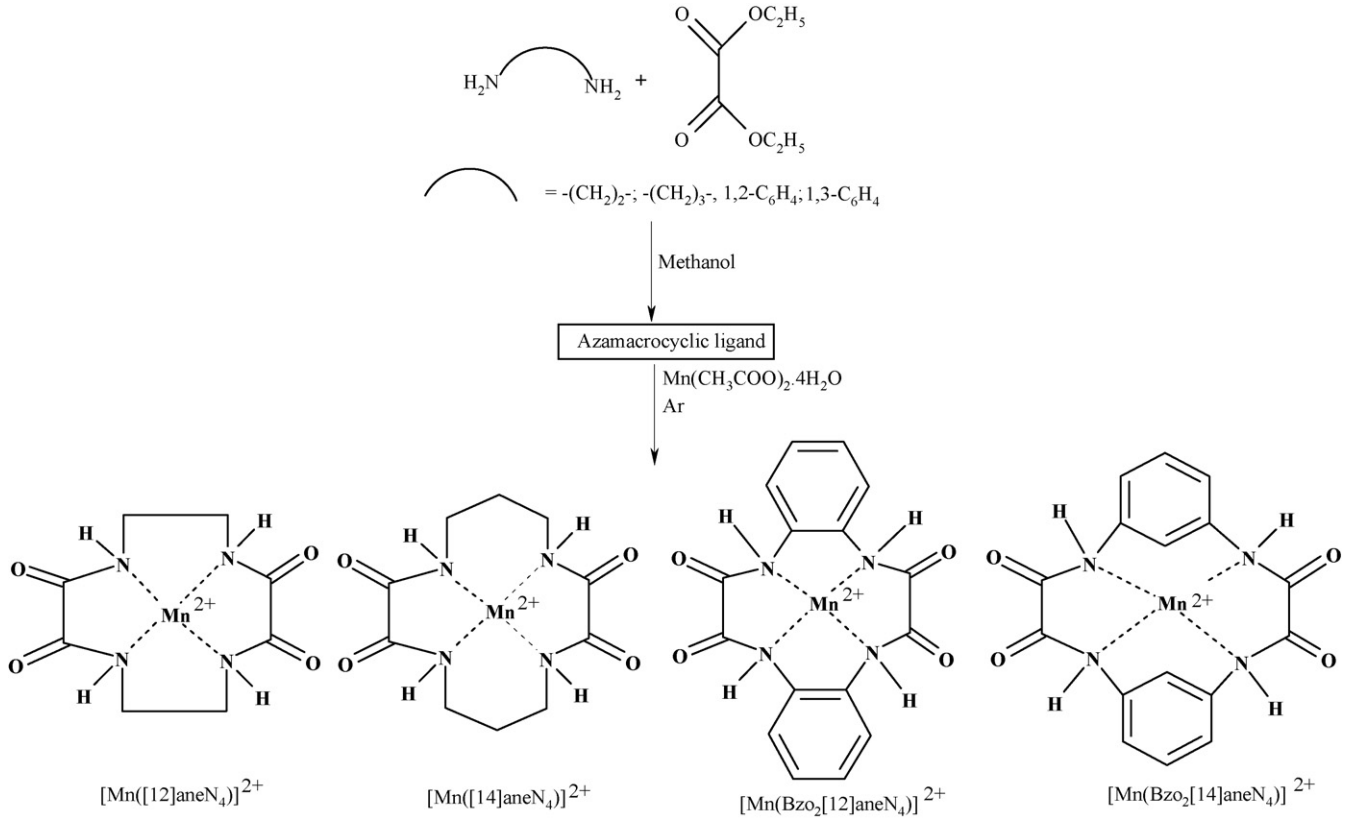

Scheme 1.

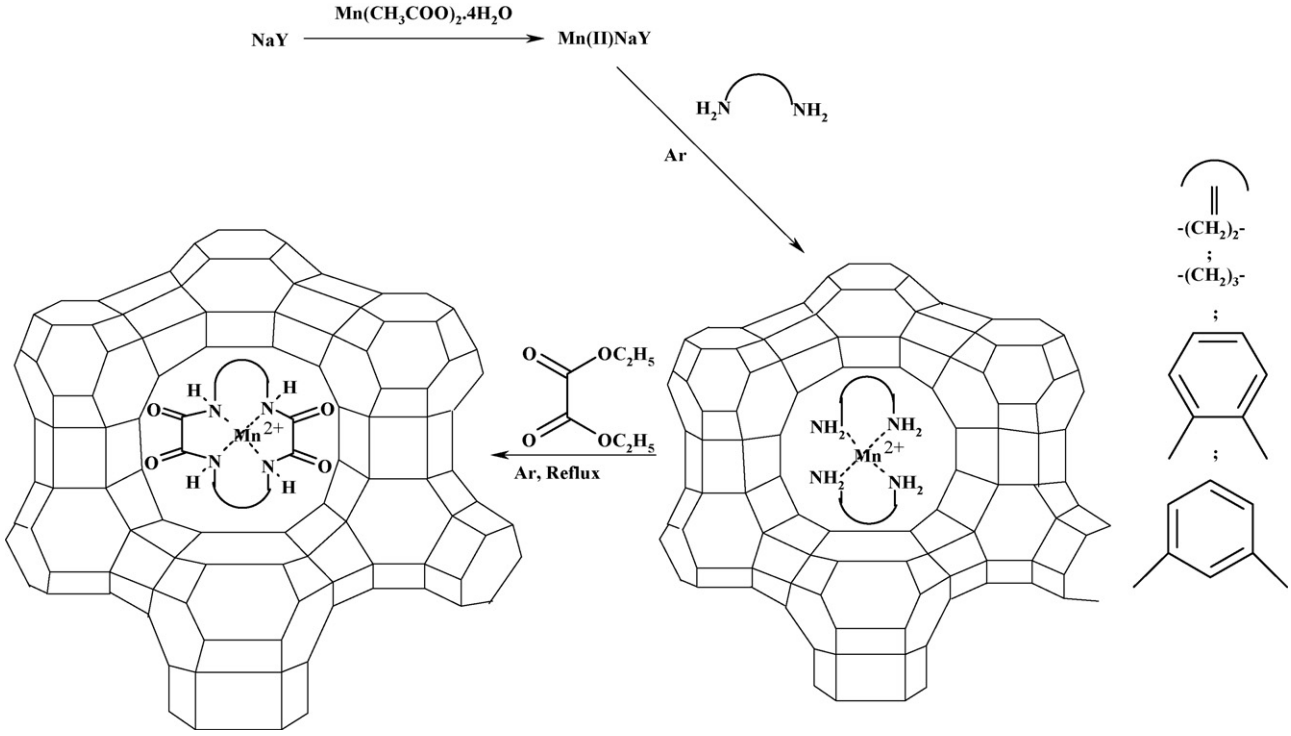

Scheme 2.

erence. The elemental analysis (carbon, hydrogen and nitrogen) of the materials was obtained from Carlo ERBA Model EA 1108 analyzer. XRD patterns were recorded by a Rigaku D-max C III, X-ray diffractometer using Ni-filtered Cu Kα radiation. Nitrogen adsorption measurements were performed at 77 K using a Coulter Ofeisorb 100CX instrument. The samples were degassed at 150 °C until a vacuum better than 10^{-3} Pa was obtained. Micropore volumes were determined by the *t*-method, a "monolayer equivalent area" was calculated from the micropore volume [7]. The stability of the encapsulated catalyst was checked after the reaction by UV–vis and possible leaching of the complex was investigated by UV–vis in the reaction solution after filtration of the zeolite. The amounts of metallocomplexes encapsulated in zeolite matrix were determined by the elemental analysis and by subtracting the amount of metallocomplex left in the solutions after the synthesis of the catalysts as determined by UV–vis spectroscopy, from the amount taken for the synthesis. Atomic absorption spectra (AAS) were recorded on a Perkin-Elmer 4100-1319 Spectrophotometer using a flame approach, after acid (HF) dissolution of known amounts of the zeolitic material and SiO_2 was determined by gravimetric analysis.

2.2. Synthesis of azamacrocyclic ligand

Azamacrocyclic ligands ([12]aneN$_4$, [14]aneN$_4$, Bzo$_2$[12]aneN$_4$ or Bzo$_2$[14]aneN$_4$) were prepared by following the procedures reported in Ref. [8]. The hot ethanolic solution (20 ml) of diethyloxalate (2.9228 g, 0.02 mol) and a hot ethanolic solution (20 ml) of diamine (0.02 mol); 1,2-diaminoethane (1.20 g), 1,3-diaminopropane (1.48 g), 1,2-diaminobenzene (2.16 g), 1,3-diaminobenzene (2.16 g); were mixed slowly with constant stirring. This mixture was refluxed for 7 h in the presence of few drops of concentrated hydrochloric acid. On cooling a solid precipitate was formed, which was filtered, washed with cold ethanol and dried under vacuum over P_4O_{10}.

2.3. Preparation of [Mn(azamac.)](ClO$_4$)$_2$

Manganese(II) sulfate monohydrate (1.69 g, 0.01 mol) dissolved in ethanol (20 ml) was reacted with an ethanol (20 ml) solution 0.01 mol of azamacrocyclic ligand ([12]aneN$_4$ (2.28 g), [14]aneN$_4$ (2.56 g), Bzo$_2$[12]aneN$_4$ (3.24 g) or Bzo$_2$[14]aneN$_4$ (3.24 g)) by refluxing for 1 h under nitrogen atmosphere. The mixture was heated at reflux for 6 h until a yellow solution resulted. The solution was cooled to room temperature and filtered to remove manganese hydroxide. Excess lithium perchlorate dissolved in methanol was added to the filtrate, and the mixture was kept in the refrigerator until yellow solid formed. The solids were filtered, washed thoroughly with cold ethanol and dried in vacuum.

2.4. Preparation of Mn(II)–NaY

Mn(II)–NaY zeolite was prepared from NaY by ion exchange using a 5 mM aqueous solution of Mn(CH$_3$COO)$_2$·4H$_2$O and 1–10 solid-to-liquid weight ratio. The mixture was heated and stirred at 90 °C for 24 h under nitrogen atmosphere. The solid was filtered, washed with hot distilled water till the filtrate was free from any manganese(II) ion (by AAS of filtrate) content

and dried for 10 h at 80 °C under vacuum. The ionic exchange degree was determined by AAS. The resulting Mn(II)–NaY zeolite containing 1.6 Mn^{2+} ions per unit cell (which corresponds to an average of Mn^{2+} every five supercages).

2.5. Preparation of $[Mn(N–N)_2]^{2+}$–NaY (N–N=diamine)

To a stirred methanol solution of Mn(II)–NaY (4 g) were added 0.37 g of diamine (1,2-diaminopropane, 1,3-diaminopropane, 1,2-diaminobenzene or 1,3-diaminobenzene) suspended in 100 ml of methanol and then refluxed for 8 h under N_2 atmosphere. The light yellow solid consisting of $[Mn(N–N)_2]^{2+}$ denoted as $[Mn(N–N)_2]^{2+}$–NaY was collected by filtration, wash with ethanol. The resulted zeolites, were Soxhlet extracted with *N*,*N*′-dimethylformamide (for 4 h) and then with ethanol (for 3 h) to remove excess unreacted diamine and any Mn(II) complexes adsorbed onto the external surface of the zeolite crystallites. The resulting light yellow solids were dried at 60 °C under vacuum for 24 h.

2.6. Preparation of $[Mn(azamac.)]^{2+}$–NaY

To a stirred methanol suspension (100 ml) of $[Mn(N–N)_2]^{2+}$–NaY (2 g) were slowly added diethyloxalate (under N_2 atmosphere). The mixture was heated under reflux condition for 24 h until a pale yellow suspension resulted. The solution was filtered and the resulting zeolites, were Soxhlet extracted with *N*,*N*′-dimethylformamide (for 4 h) and then with ethanol (for 4 h) to remove excess unreacted products from amine-ester condensation and any manganese(II) complexes adsorbed onto the external surface of the zeolite crystallites. The resulting pale yellow solids were dried at 70 °C under vacuum for 12 h. The remaining [bis(diamine)manganese(II)] ions in zeolite were removed by exchanging with aqueous 0.1 M $NaNO_3$ solutions. The stability of the encapsulated catalyst was checked after the reaction by UV–vis and possible leaching of the complex was investigated by UV–vis in the reaction solution after filtration of the zeolite. The amounts of Mn(II) complexes encapsulated in zeolite matrix were determined by the elemental analysis and by subtracting the amount of Mn(II) complex left in the solutions after the synthesis of the catalysts as determined by UV–vis spectroscopy, from the amount taken for the synthesis.

2.7. Oxidation of cyclohexene; general procedure

A mixture of 1.02×10^{-5} mol catalyst, 25 ml CH_2Cl_2 and 10 mmol cyclohexene was stirred under nitrogen in a 50-ml round-bottom flask equipped with a condenser and a dropping funnel at 40 °C for 30 min. Then 16 mmol of TBHP solution in CH_2Cl_2 was added. The resulting mixture was then refluxed for 8 h under N_2 atmosphere. After filtrating and washing with solvent, the filtrate was concentrated on a rotary evaporator and then subjected to GC analysis.

3. Results and discussion

3.1. Synthesis of complexes

Manganese(II) reacted with azamacrocyclic ligands in presence of $LiClO_4$ to yield the cationic complexes, $[Mn([12]aneN_4)](ClO_4)_2$, $[Mn([14]aneN_4)](ClO_4)_2$, $[Mn(Bzo_2[12]aneN_4)](ClO_4)_2$ and $[MnBzo_2[14]aneN_4)](ClO_4)_2$ (Scheme 1). Acetonitrile solutions of these complexes were conductive (Table 1). Unfortunately, we could not grow any single crystals suitable for X-ray crystallographic studies. The Mn complexes described herein all involve the ligands functioning as a neutral, tetradentate chelate through its N–H groups. The structures of complexes demonstrate the considerable inflexibility in the conformations that multidentate ligands can adopt (Scheme 1).

The molar conductance values of tetraaza macrocyclic complexes (~240 Ω^{-1} mol^{-1} cm^2) and measured correspond to 1:2 electrolytes. IR spectrum of the ligands does not exhibit any band corresponding for the free primary diamine and ketonic group. Four new bands, were appeared in the spectrum of ligand [9] in the regions 1651, 1518, 1226 and 762 cm^{-1} are assignable to amide-I ν(C=O), amide-II [ν(C–N) + δ(N–H)], amide-III [δ(N–H)] and amide-IV [φ(C=O)] bands, respectively. This supports the macrocyclic nature of the ligand. A single sharp band observed at 3300 cm^{-1}, may be due to ν(N–H) of the secondary amino group [10]. On complexation the position of ν(N–H) bands shifted to lower frequency compared to the macrocyclic ligand and a new medium intensity band appears at 418–490 cm^{-1} attribute to ν(Mn–N), it provide, strong evidence for the involvement of nitrogen in coordination. IR spectrum indicates that the ligand act as tetradentate coordinating through nitrogen [N_4].

The electronic spectra of all the complexes, in DMF, show intraligand transition bands at 320 and 280 nm, while the MLCT bands fall near 350 nm. The position of the MLCT band depends on functional group amide or amine. As expected for Mn(II) complexes, d–d transition bands are not observed in dilute solution because of their being doubly forbidden.

3.2. Heterogenisation of complexes

The heterogenisation of homogeneous catalysts is a field of continuing interest: indeed, although some of the organometallic complexes exhibit remarkable catalytic properties (activities and selectivity), they are unsuitable to separate intact, from the reaction medium making difficult their reuse and contaminating the reaction products. Thus, the heterogenisation is always a toxicological and environmental challenge; moreover, it has an economical significance unless the activity of the homogeneous catalysts was exceptionally high. I have made the heterogenisation by encapsulating or encaging the catalyst in the voids of a nanoporous inorganic solid (zeolite-Y) (Scheme 2). The objective, clearly, is to improve the stability of the metal complex under the reaction conditions by preventing the catalytic species from dimerising or aggregation, and to tune the selectivity of the reaction using the walls of the pores of the solid via steric constraints. In this approach,

Table 1
Elemental analysis, vibrations parameters and some physical properties for ligands and azamacrocyclic manganese(II) complexes

Complex	Calculated (found)					Λ_M[a] (Ω^{-1} cm^2 mol^{-1})	μ_{eff} (MB)	IR (KBr, cm^{-1})	
	C (%)	H (%)	N (%)	C/N	Mn (%)			ν(C=O)	ν(N–H)
[12]aneN$_4$	42.11 (41.92)	5.30 (5.18)	24.54 (24.66)	1.72 (1.70)	–	–	–	1663	3314
[Mn([12]aneN$_4$)](ClO$_4$)$_2$	19.92 (19.70)	2.49 (2.38)	11.62 (11.80)	1.71 (1.67)	11.41 (11.27)	250	5.93	1659	3305
[14]aneN$_4$	46.87 (46.67)	6.29 (6.13)	21.85 (21.99)	2.14 (2.12)	–	–	–	1651	3298
[Mn([14]aneN$_4$)](ClO$_4$)	23.54 (23.36)	3.14 (3.02)	10.98 (11.07)	2.14 (2.11)	10.77 (10.60)	248	5.92	1644	3290
Bzo$_2$[12]aneN$_4$	59.26 (59.04)	3.73 (3.52)	17.27 (17.39)	3.43 (3.40)	–	–	–	1678	3325
[Mn(Bzo$_2$[12]aneN$_4$)](ClO$_4$)	33.23 (33.07)	2.08 (1.93)	9.69 (9.75)	3.43 (3.39)	9.50 (9.40)	240	5.91	1675	3318
Bzo$_2$[14]aneN$_4$	59.26 (59.00)	3.73 (3.48)	17.27 (17.41)	3.43 (3.39)	–	–	–	1675	3318
[Mn(Bzo$_2$[14]aneN$_4$)](ClO$_4$)	33.23 (33.07)	2.08 (1.95)	9.69 (9.80)	3.43 (3.37)	9.50 (9.37)	242	5.92	1668	3310

[a] In acetonitrile solutions.

the metal is introduced in the nanopores of a solid via cation exchange.

The azamacrocyclic ligands are then introduced under the conditions indicated in Section 2 for complex formation, according to the template condensation strategy for the encapsulation of metal complexes inside the nanocavities of zeolite hosts. There, complexation occurs and the resulting complexes are too bulky and rigid to be able to leave the cavities again. Uncomplexed ligands and complexes formed at the external surface of the zeolite crystallites have to be removed as far as possible. Identity of the complex has been established by spectroscopic methods and IR and DRS of encapsulated complexes that are coincided with that are recorded for homogeneous complexes. The complex formed is like a "ship-in-bottle", confined in the supercages of the zeolite: this explains greater stability of these catalysts as compared with the same complexes in solution. No metal leaching is observed, as long as the complex is exclusively inside the pores.

The chemical compositions confirmed the purity and stoichiometry of the neat and encapsulated complexes. The chemical analysis of the samples revealed the presence of organic matter with a C/N ratio roughly similar to that for neat complexes. The percentage of manganese(II) contents estimated before and after encapsulation by atomic absorption spectroscopy. The manganese(II) ion contents estimated after encapsulation are only due to the presence of manganese(II) complexes in nanopores of zeolite-Y. The Si and Al contents in Mn(II)–NaY and the zeolite complexes are almost in the same ratio as in the parent zeolite. This indicates little changes in the zeolite framework due to the absence of dealumination in metal ion exchange. The parent NaY zeolite has Si/Al molar ratio of 2.53 which corresponds to a unit cell formula $Na_{56}[(AlO_2)_{56}(SiO_2)_{136}]$. The unit cell formula of metal-exchanged zeolites shows a manganese dispersion of 11.4 moles per unit cell ($Na_{33.8}Mn_{11.4}[(AlO_2)_{56}(SiO_2)_{136}]\cdot nH_2O$). The analytical data of each complex indicates Mn:C:N molar ratios almost close to those calculated for the mononuclear structure. Elemental analysis and spectroscopic data's (Tables 1 and 2) show that all of the neat complexes have square–planar coordinated structure.

IR spectroscopy provided information on the integrity of the encapsulated complexes, as well as the crystallinity of the host zeolite. The IR bands of all encapsulated complexes were weak due to their low concentration in the zeolite. Mn(II) complexes encapsulated in the zeolite cages did not show any significant shift in N–H or C=O stretching modes. We did not notice any appreciable changes in the frequencies of Mn complexes after incorporation into zeolite matrix. The major FTIR bands of the catalysts are tabulated in Table 2. The diffuse reflectance spectra of Mn(II) complexes are almost identical before and after encapsulation, indicating that the complexes maintain their geometry even after encapsulation without significant distortion.

The X-ray diffractograms of the catalysts containing the Mn(II) complexes did not reveal any significant difference from those of NaY. The encapsulation of the manganese complexes inside the zeolite cavities is indicated by the absence of extraneous material by scanning electron microscopy (SEM).

Table 2
Chemical composition and IR stretching frequencies (as KBr pellets) of nanopores of zeolite encapsulated azamacrocyclic manganese(II) complexes

Sample	C (%)	H (%)	N (%)	C/N	Si (%)	Al (%)	Na (%)	Mn (%)	Si/Al	$\nu_{C=O}$ (cm^{-1})	ν_{N-H} (cm^{-1})
NaY	–	–	–	–	21.76	8.60	7.50	–	2.53	–	–
Mn(II)–NaY	–	–	–	–	22.08	8.73	3.34	2.58	2.53	–	–
$[Mn([12]aneN_4)]^{2+}$–NaY	3.74	1.53	2.58	1.45	21.14	8.36	5.34	2.34	2.53	1661	3308
$[Mn([14]aneN_4)]^{2+}$–NaY	3.76	1.55	1.91	1.97	21.12	8.35	5.33	2.31	2.53	1647	3294
$[Mn(Bzo_2[12]aneN_4)]^{2+}$–NaY	3.80	1.57	1.19	3.20	21.10	8.34	5.29	2.28	2.53	1679	3321
$[Mn(Bzo_2[14]aneN_4)]^{2+}$–NaY	3.81	1.58	1.20	3.18	21.08	8.33	5.30	2.29	2.53	1678	3314

Both X-ray diffraction and SEM indicated that zeolites with good crystallinity can be obtained during the encapsulation of $[Mn(azamac.)]^{2+}$ complexes by the one pot template condensation reaction.

The surface area and pore volume of the catalysts are shown in Table 3. The inclusion of Mn(II) azamacrocyclic complexes dramatically reduces the adsorption capacity and the surface area of the zeolite. It has been reported [11] that the BET surface area of X and Y zeolite containing phthalocyanine complexes are typically less than 100 $m^2\,g^{-1}$. The lowering of the pore volume and surface area indicate the presence of azamacrocyclic manganese(II) complexes within the cavities of the zeolites and not on the external surface.

Table 3
Surface area and pore volume data of azamacrocyclic manganese(II) complexes encapsulated in nanopores of zeolite-Y

Sample	Surface area[a] (m^2/g)	Pore volume[b] (ml/g)
NaY	545	0.31
Mn(II)–NaY	535	0.30
$[Mn([12]aneN_4)]^{2+}$–NaY	498	0.27
$[Mn([14]aneN_4)]^{2+}$–NaY	484	0.26
$[Mn(Bzo_2[12]aneN_4)]^{2+}$–NaY	469	0.23
$[Mn(Bzo_2[14]aneN_4)]^{2+}$–NaY	465	0.22

[a] Surface area is the "monolayer equivalent area" calculated as explained in Ref. [7].
[b] Calculated by the *t*-method.

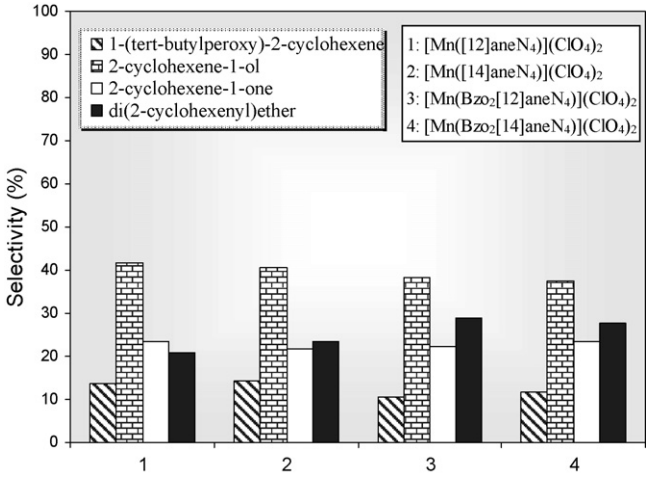

Fig. 1. Oxidation products distribution in acetonitrile with $[Mn(azamac.)]^{2+}$/TBHP.

3.3. Catalytic activity

Results of Table 4 show the catalytic activity of homogeneous catalysts. Comparing between neat and HGNM (Tables 4–7 and Figs. 1 and 2) complexes as catalyst evidence that neat complexes gave higher conversion of cyclohexene than their corresponding HGNM. For homogeneously catalyzed reactions, the termination of catalytic cycle may occur because of two factors, due to the formation of Mn–O–Mn species, or due to the oxidative degradation of metal complexes. This was confirmed

Table 4
Oxidation of cyclohexene with TBHP catalyzed by manganese(II) complexes in CH_2Cl_2

Catalyst	Conversion (%)	Selectivity (%)			
		Peroxide[a]	Alcohol[b]	Ketone[c]	Ether[d]
$[Mn([12]aneN_4)](ClO_4)_2$	78.94	13.85	34.75	23.54	20.86
$[Mn([14]aneN_4)](ClO_4)_2$	76.80	14.19	40.53	21.76	23.52
$[Mn(Bzo_2[12]aneN_4)](ClO_4)_2$	94.75	10.44	38.31	22.30	28.95
$[Mn(Bzo_2[12]aneN_4)](ClO_4)_2$[e]	70.32	21.85	49.60	20.56	7.99
$[Mn(Bzo_2[12]aneN_4)](ClO_4)_2$[f]	90.56	32.84	34.26	27.54	5.36
$[Mn(Bzo_2[12]aneN_4)](ClO_4)_2$[g]	43.27	35.89	28.57	31.42	4.12
$[Mn(Bzo_2[14]aneN_4)](ClO_4)_2$	90.17	11.65	37.29	23.41	27.65

[a] 1-(*tert*-Butylperoxy)-2-cyclohexene.
[b] 2-Cyclohexene-1-ol.
[c] 2-Cyclohexene-1-one.
[d] Di(2-cyclohexenyl)ether.
[e] Catalyst = 0.5×10^{-5} mol.
[f] Catalyst = 2.04×10^{-5} mol.
[g] Catalyst = 4.08×10^{-5} mol.

Table 5
Oxidation of cyclohexene with TBHP catalyzed by HGNM in CH_2Cl_2

Catalyst	Conversion (%)	Selectivity (%)			
		Peroxide[a]	Alcohol[b]	Ketone[c]	Ether[d]
Mn(II)–NaY	51.43	9.78	8.72	33.99	47.51
$[Mn([12]aneN_4)]^{2+}$–NaY	68.51	3.40	4.80	9.10	82.7
$[Mn([14]aneN_4)]^{2+}$–NaY	65.25	4.81	5.21	5.51	84.50
$[Mn(Bzo_2[12]aneN_4)]^{2+}$–NaY	80.34	1.30	2.01	3.29	93.40
$[Mn(Bzo_2[12]aneN_4)]^{2+}$–NaY[e]	79.14	1.45	2.27	3.19	93.09
$[Mn(Bzo_2[12]aneN_4)]^{2+}$–NaY[f]	78.22	1.82	3.10	2.87	92.21
$[Mn(Bzo_2[12]aneN_4)]^{2+}$–NaY[g]	77.25	2.31	3.56	2.77	91.36
$[Mn(Bzo_2[14]aneN_4)]^{2+}$–NaY	76.42	3.18	2.98	3.74	90.10

[a] 1-(*tert*-Butylperoxy)-2-cyclohexene.
[b] 2-Cyclohexene-1-ol.
[c] 2-Cyclohexene-1-one.
[d] Di(2-cyclohexenyl)ether.
[e] First reuse.
[f] Second reuse.
[g] Third reuse.

Table 6
Oxidation of cyclohexene with TBHP catalyzed by HGNM in C_2H_5OH

Catalyst	Conversion (%)	Selectivity (%)			
		Peroxide[a]	Alcohol[b]	Ketone[c]	Ether[d]
Mn(II)–NaY	57.1	13.96	19.38	–	66.66
$[Mn([12]aneN_4)]^{2+}$–NaY	70.49	5.93	9.53	–	84.54
$[Mn([14]aneN_4)]^{2+}$–NaY	69.11	6.62	7.46	–	85.92
$[Mn(Bzo_2[12]aneN_4)]^{2+}$–NaY	84.51	2.24	2.66	–	95.10
$[Mn(Bzo_2[14]aneN_4)]^{2+}$–NaY	78.52	3.45	3.35	–	93.2

[a] 1-(*tert*-Butylperoxy)-2-cyclohexene.
[b] 2-Cyclohexene-1-ol.
[c] 2-Cyclohexene-1-one.
[d] Di(2-cyclohexenyl)ether.

by taking the IR spectra of the solid after catalytic reaction. The IR spectra of these solids are very much different from that of the IR spectra of the parent compounds. To improve the stability of the metal complex under the reaction conditions we have heterogenised the complexes by preventing the catalytic species from dimerising or aggregation, and to tune the selectivity of the reaction using the walls of the nanopores of the solid via steric effects.

The most important advantage of heterogeneous catalysis over its homogeneous counterpart is a high increasing of

Table 7
Oxidation of cyclohexene with TBHP catalyzed by HGNM in CH_3CN

Catalyst	Time (h)	Conversion (%)	Selectivity (%)			
			Peroxide[a]	Alcohol[b]	Ketone[c]	Ether[d]
Mn(II)–NaY	8	56.84	21.38	6.11	6.45	66.10
$[Mn([12]aneN_4)]^{2+}$–NaY	8	73.92	11.94	4.56	8.33	75.17
$[Mn([14]aneN_4)]^{2+}$–NaY	8	72.12	12.04	3.47	7.25	77.24
$[Mn(Bzo_2[12]aneN_4)]^{2+}$–NaY	2	24.72	29.38	13.80	4.70	52.12
$[Mn(Bzo_2[12]aneN_4)]^{2+}$–NaY	4	51.65	19.75	10.38	5.39	64.48
$[Mn(Bzo_2[12]aneN_4)]^{2+}$–NaY	6	75.39	13.52	7.54	6.53	72.41
$[Mn(Bzo_2[12]aneN_4)]^{2+}$–NaY	8	88.45	7.35	4.08	8.44	80.13
$[Mn(Bzo_2[12]aneN_4)]^{2+}$–NaY	10	89.31	6.21	2.17	9.75	81.87
$[Mn(Bzo_2[12]aneN_4)]^{2+}$–NaY	12	90.46	4.65	1.27	12.36	81.72
$[Mn(Bzo_2[14]aneN_4)]^{2+}$–NaY	8	85.17	7.46	8.95	9.39	74.2

[a] 1-(*tert*-Butylperoxy)-2-cyclohexene.
[b] 2-Cyclohexene-1-ol.
[c] 2-Cyclohexene-1-one.
[d] Di(2-cyclohexenyl)ether.

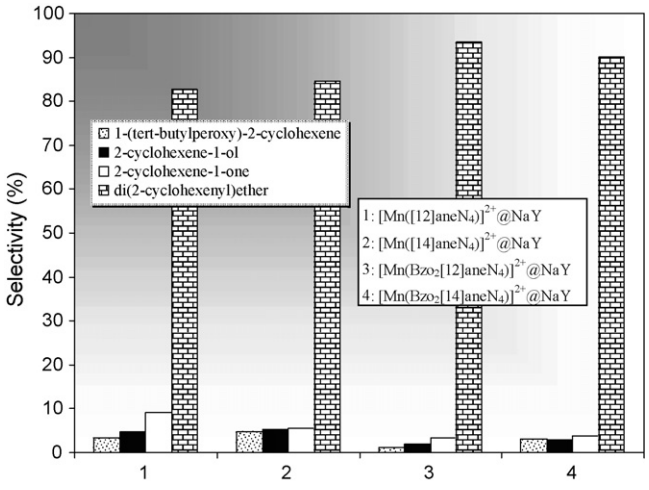

Fig. 2. Oxidation products distribution in dichloromethane with $[Mn(azamac.)]^{2+}$–NaY/TBHP.

the complex stability in the reaction media and the possibility of reusing the catalyst after reaction by simple filtration (Tables 5–7). The catalyst could be reused at least three times without neither loss of selectivity nor activity with catalyst loading as low as 1 mol%. While the oxidation of cyclohexene continued in presence of the catalyst, there was no further significant conversion when the catalyst was removed from the reaction system (Table 5). This conclusion was independently confirmed by the absence of manganese in the filtrate (atomic absorption spectroscopy).

The effect of Mn(II) complexes included in zeolite-Y were studied on the oxidation of cyclohexene with TBHP in CH_2Cl_2 and the results are shown in Table 5. As is shown in Fig. 1, the allylic oxidation has occurred with the formation of 2-cyclohexene-1-ol, 2-cyclohexen-1-one, 1-*tert*-butylperoxy-2-cyclohexene and di-2-cyclohexenylether. The activity of Mn(II)–NaY catalyst has also been included in Table 5 to compare the effect of the ligand on the activity of catalyst. Increase of conversion percentage from 51.43% to 80.34% compared to Mn(II)–Y with $[Mn(Bzo_2[12]aneN_4)]^{2+}$–NaY indicates that the existence of ligand has increased the activity of catalyst by a factor of 1.56. From the results indicated in Tables 5–7, it is evident that ether has been formed selectively in the presence of all catalysts although $[Mn(Bzo_2[12]aneN_4)]^{2+}$–NaY shows the most tendency towards the formation of this product.

In the present study, it is observed that compared to the Mn(II)–NaY catalyst system, the ketone yield is lower and the reaction has led mostly to the formation of alcohol and ether. As was suggested before, the ether product has arisen from the etherification of 2-cyclohexene-1-ol [12]. This idea was confirmed by using 2-cyclohexene-1-ol instead of cyclohexene as starting material and observed the formation of the ether as the main product under the reaction conditions. That the acidity of zeolite catalyst has catalyzed the formation of di-2-cyclohexenylether was ruled out since there was hardly any reaction in the absence of oxidant under my reaction conditions. Therefore, the combination of zeolite catalyst and oxidant has been responsible for the conversion of alcohol to ether product.

To investigate the role of solvent on the fate of reaction and product distribution, I carried out the reaction in two groups of protic and aprotic solvents. The results are given in Tables 5–7. From these results, it is evident that polar protic solvent such as ethanol and polar aprotic solvent such as acetonitrile have presented the best media for $[Mn(Bzo_2[12]aneN_4)]^{2+}$–NaY catalyst, since the conversion has occurred about 95%.

As mentioned before [13], higher activity of $[Mn(Bzo_2[12]aneN_4)]^{2+}$–NaY complex might be attributed to the higher activity of aromatic ligand and its more active cation radical intermediate with respect to the aliphatic ligand system ethylenediamine with the conversion percentage of 84.51% in ethanol. Lower activity of $[Mn([14]aneN_4)]^{2+}$–NaY can be accounted for by the substantial steric hindrance of propylene groups that prevent the approaching oxidant towards the central metal of the catalyst.

As shown in Tables 5–7, $[Mn(Bzo_2[12]aneN_4)]^{2+}$–NaY shows the highest activity in all the different solvent systems. Moreover, the ether product has been selectively formed under the effect of this catalyst from 79% to 95.10%. Since ether has arisen from the etherification of 2-cyclohexene-1-ol (see above), and maximum percentage resulted in ethanol, it can be concluded that the catalyst $[Mn(Bzo_2[12]aneN_4)]^{2+}$–NaY presents the strongest acidic medium in this reaction.

The effect of time on the reactivity of catalysts is shown in Table 7. Acetonitrile was selected as solvent for this experiment because all four products have been formed under this solvent medium effect. Table 7 shows that during 8 h, maximum conversion of starting material takes place with all catalyst systems.

The results clearly suggest that $[Mn(Bzo_2[12]aneN_4)]^{2+}$–NaY efficiently catalyses conversion of cyclohexene to di-2-cyclohexenylether. The more activity of $Bzo_2[12]aneN_4$ system has clearly arisen from the existence of electron donating ligand which facilitate the electron transfer rate, a process that has previously observed by us in other oxidation reactions [4,13–16]. All conversions efficiency with high selectivity obtained in this study is significantly higher than that obtained using metal containing porous and nonporous materials [4,13–16].

4. Conclusion

Tetraaza 12- and 14-membered macrocyclic ligands and their manganese complexes have been encapsulated in the nanopores of zeolite-Y. The resulting catalysts have been characterized by various spectroscopic (IR, DRS, UV–Vis), elemental analysis, etc. The oxidation of cyclohexene with TBHP and Mn complexes included in zeolite-Y selectively affords di-2-cyclohexenylether as the main product. My studies show that the oxidation exclusively occurs on the allylic position. We believe that the combination of a catalyst and oxidant system like $[Mn(Bzo_2[12]aneN_4)]^{2+}$–NaY and TBHP in commonly and highly used solvent like ethanol provides a simple route to the allylic site oxidation of cyclohexene. Studies on other olefins are currently under investigation in our laboratory and we believe that the observation of similar results on other olefins is not unexpected.

Acknowledgment

Author is grateful to Council of University of Kashan for providing financial support to undertake this work.

References

[1] F. Schüth, W. Schmidt, Adv. Mater. 14 (2002) 629;
F. Schuth, K. Sing, J. Weitkamp (Eds.), Handbook of Porous Solids, vols. I–V, Wiley–VCH, Weinheim, 2002 (and references therein).
[2] A.K. Cheetham, G. Ferey, T. Loiseau, Angew. Chem. Int. Ed. 38 (1999) 3268.
[3] D. Kaucky, A. Vondrova, J. Dedecek, B. Wichterlova, J. Catal. 194 (2000) 318.
[4] M. Hartman, Angew. Chem. Int. Ed. 39 (2000) 888;
M. Salavati-Niasari, Inorg. Chem. Commun. 9 (2006) 628;
M. Salavati-Niasari, F. Davar, Inorg. Chem. Commun. 9 (2006) 263;
M. Salavati-Niasari, F. Davar, Inorg. Chem. Commun. 9 (2006) 304;
M. Salavati-Niasari, J. Mol. Catal. A: Chem. 245 (2006) 192;
M. Salavati-Niasari, Chem. Lett. 34 (2005) 1444;
M. Salavati-Niasari, J. Mol. Catal. A: Chem. 229 (2005) 159;
M. Salavati-Niasari, Chem. Lett. 34 (2005) 244;
M. Salavati-Niasari, Inorg. Chem. Commun. 8 (2005) 174;
M. Salavati-Niasari, Inorg. Chem. Commun. 7 (2004) 963;
M. Salavati-Niasari, J. Mol. Catal. A: Chem. 217 (2004) 87.
[5] M.R. Maurya, S.J.J. Titinchi, S. Chand, J. Mol. Catal. A: Chem. 214 (2004) 257;
M.R. Maurya, S.J.J. Titinchi, S. Chand, J. Mol. Catal. A: Chem. 201 (2003) 119;
M.R. Maurya, S.J.J. Titinchi, S. Chand, J. Mol. Catal. A: Chem. 193 (2003) 165;
M.R. Maurya, S.J.J. Titinchi, S. Chand, I.M. Mishra, J. Mol. Catal. A: Chem. 180 (2002) 201;
I.W.C.E. Arends, R.A. Sheldon, Appl. Catal. A: Gen. 212 (2001) 175.
[6] P.P. Knops-Gerrits, F. Thibault-Starzyk, P.A. Jacobs, Stud. Surf. Sci. Catal. 84 (1994) 1411;
K.J. Balkus Jr., A.K. Khanrnamedova, K.M. Dixon, F. Bedioui, Appl. Catal. A: Gen. 143 (1996) 159;
D. Chatterjee, A. Mitr, J. Mol. Catal. A: Chem. 144 (1999) 363.
[7] S.W. Wang, H. Everett, R.A.W. Haul, L. Moscou, R.A. Pierotti, J. Rouquerol, T. Siemieniewska, Pure Appl. Chem. 57 (1985) 603;
A. Lineares-Solano, in: J.L. Figueiredo, J.A. Moulijn (Eds.), Carbon and Coal Gasification, M. Nijhoff, M.A. Dordrecht, 1986, p. 137.
[8] S. Chandra, L.K. Gupta, Spectrochim. Acta A 61 (2005) 2139.
[9] M. Shakir, O.S.M. Nasman, A.K. Mohamed, S.P. Varkey, Ind. J. Chem. 35A (1996) 770.
[10] U.K. Pandey, S.K. Sengupta, S.C. Tripathi, Polyhedron 6 (1987) 1611.
[11] K.J. Balkus Jr., A.G. Gabrielov, J. Inclusion Phenom. Mol. Recogn. Chem. 21 (1995) 173.
[12] S. Kim, K.N. Chung, J. Org. Chem. 52 (1987) 3917.
[13] M. Salavati-Niasari, H. Banitaba, J. Mol. Catal. A: Chem. 201 (2003) 43;
M. Salavati-Niasari, A. Amiri, Appl. Catal. A: Gen. 290 (2005) 46;
M. Salavati-Niasari, P. Salemi, F. Davar, J. Mol. Catal. A: Chem. 238 (2005) 215;
M. Salavati-Niasari, S. Hydarzadeh, J. Mol. Catal. A: Chem. 237 (2005) 254.
[14] R.F. Parton, I.F.J. Vankelecom, M.J.A. Casselman, C.P. Bezoukhanova, J.B. Uytterhoeven, P.A. Jacobs, Nature 370 (1994) 541.
[15] R.F. Parton, C.P. Bezoukhanova, F. Thibault-Starzyk, R.A. Reynders, P.J. Grobet, P.A. Jacobs, Stud. Surf. Sci. Catal. 84 (1994) 813.
[16] K.J. Balkus Jr., M. Eissa, R. Lavado, Stud. Surf. Sci. Catal. 94 (1995) 713;
K.J. Balkus Jr., M. Eissa, R. Lavado, J. Am. Chem. Soc. 117 (1995) 10753.